RAA 2014 Vol. **14** No. **5**, 601–609 doi: 10.1088/1674–4527/14/5/009
http://www.raa-journal.org *http://www.iop.org/journals/raa*

Research in Astronomy and Astrophysics

A method for calculating probability of collision between space objects *

Xiao-Li Xu and Yong-Qing Xiong

[1] Purple Mountain Observatory, Chinese Academy of Sciences, Nanjing 210008, China; *xlxu@pmo.ac.cn*
[2] Key Laboratory of Space Object and Debris Observation, Chinese Academy of Sciences, Nanjing 210008, China

Received 2013 September 2; accepted 2013 November 11

Abstract A method is developed to calculate probability of collision. Based on geometric features of space objects during the encounter, it is reasonable to separate the radial orbital motions from those in the cross section for most encounter events that occur in a near-circular orbit. Therefore, the probability of collision caused by differences in both altitude of the orbit in the radial direction and the probability of collision caused by differences in arrival time in the cross section are calculated. The net probability of collision is expressed as an explicit expression by multiplying the above two components. Numerical cases are applied to test this method by comparing the results with the general method. The results indicate that this method is valid for most encounter events that occur in near-circular orbits.

Key words: methods: analytical — reference systems — catalogs — space vehicles — celestial mechanics

1 INTRODUCTION

Currently, a very large number of space debris are orbiting in near earth orbit below 2000 km which could potentially threaten space missions and spacecrafts (Sun & Zhao 2013). Collision events could disturb or damage spacecrafts as well as produce new debris, leading to a vicious cycle in the space environment. Although a collision event between two space objects rarely happens, several collision accidents have already been confirmed. In order to prevent space collision events, effective collision risk assessment and avoidance maneuvers have been carried out (Akella & Alfriend 2000; Klinkrad et al. 2005; Francois & Eloy 2008).

The earliest risk criterion was the exclusion volume method (Leleux et al. 2002). An exclusion volume surrounding the spacecraft is specified, and an alarm is raised if any object penetrates the exclusion volume. However, this method is too conservative and triggers a high number of false alarms. Therefore, the probability threshold method was proposed (Kelly & Picciotto 2005); when a probability threshold is set, an alarm is triggered if the calculated probability of collision exceeds this threshold. This approach reduces the number of false alarms and thus is more rational than the exclusion volume method. Many efforts have been dedicated to effectively calculating the probability of collision, and significant progress has been made in recent years. To calculate the probability of

* Supported by the National Natural Science Foundation of China.

collision between two objects, covariance models for both objects should be applied. It is permissible to combine the error covariance matrices for two orbiting objects to obtain a relative covariance matrix as long as they are represented in the same frame (Chan 1997). The combined covariance matrix has an associated three-dimensional probability density function (PDF) that represents the relative uncertainty in position of the two objects. Since most encounters between space objects occur at high relative velocities, calculating the probability of collision can be reduced to a two-dimensional integral over a circular region in a plane normal to the relative velocity vector, referred to as the encounter frame (Akella & Alfriend 2000). Patera (2001) further developed an approach, which reduces the calculation to a single closed-path integral, to compute probability of collision between two irregular objects. Bai & Chen (2008, 2009) also developed one method based on geometry compression method and coordinate rotation, in which the probability of collision is expressed as an explicit function of geometry in the encounter. At present, the probability threshold method has been widely adopted to assess collision risks for space objects.

The general method for calculating probability of collision involves a projection from a three-dimensional PDF to a two-dimensional one. The initial state vectors of two objects in the inertial frame are given by $\boldsymbol{r}_1$ and $\boldsymbol{r}_2$, and their corresponding error covariance matrices in the local frame are defined as $\boldsymbol{C}_1$ and $\boldsymbol{C}_2$. The transformation matrices from the local to the inertial frame are given by $\boldsymbol{P}_1$ and $\boldsymbol{P}_2$, respectively. The respective error covariance matrices in the local frame can be transformed to the ones in the inertial frame in the usual manner

$$\begin{aligned} \boldsymbol{C}_{1\mathrm{I}} &= \boldsymbol{P}_1 \boldsymbol{C}_1 \boldsymbol{P}_1^{-1}, \\ \boldsymbol{C}_{2\mathrm{I}} &= \boldsymbol{P}_2 \boldsymbol{C}_2 \boldsymbol{P}_2^{-1}. \end{aligned} \tag{1}$$

Because the errors in position of the two objects are uncorrelated, the error covariance matrices are combined to obtain the relative error covariance matrix in the inertial frame

$$\boldsymbol{C}_{\mathrm{I}} = \boldsymbol{C}_{1\mathrm{I}} + \boldsymbol{C}_{2\mathrm{I}}. \tag{2}$$

Then the relative position and velocity are needed to define the encounter frame whose z-axis is parallel to the relative velocity vector. The transformation from the inertial to the encounter frame given by $\boldsymbol{U}$ is used to derive the relative position vector and error covariance matrix in the encounter frame

$$\begin{aligned} \Delta \boldsymbol{r}_e &= \boldsymbol{U}\boldsymbol{r}_2 - \boldsymbol{U}\boldsymbol{r}_1, \\ \boldsymbol{C}_e &= \boldsymbol{U}\boldsymbol{C}_I\boldsymbol{U}^{-1}. \end{aligned} \tag{3}$$

The probability of collision in the encounter frame is expressed as

$$P = \frac{1}{\sqrt{(2\pi)^3 |\boldsymbol{C}_e|}} \iiint_V \exp\left\{-\frac{1}{2}\Delta \boldsymbol{r}_e^{\mathrm{T}} \boldsymbol{C}_e^{-1} \Delta \boldsymbol{r}_e\right\} \mathrm{d}V. \tag{4}$$

Because most encounters have high relative velocities, the relative position vector is orthogonal to the relative velocity vector when two objects are at the closest point of approach (CPA) (Chan 1997). Therefore, calculating the probability of collision can be reduced to a two-dimensional integral over a circular region in the encounter frame

$$P = \frac{1}{2\pi\sqrt{|\boldsymbol{C}_e'|}} \iint_{x^2+y^2 \le R^2} \exp\left\{-\frac{1}{2}\Delta \boldsymbol{r}_e'^{\mathrm{T}} \boldsymbol{C}_e'^{-1} \Delta \boldsymbol{r}_e'\right\} \mathrm{d}x\mathrm{d}y. \tag{5}$$

From Equation (5), we can see that probability of collision depends on the relative position, error covariance matrix and size of both objects. It has to be calculated numerically in light of this implicit expression, and some geometric features of the encounter are implied. The general

method for probability of collision provides sufficiently accurate results, but does not reveal the direct connection between probability of collision and geometry of the encounter.

Since the sensitivity to probability of collision during the encounter is significant for devising strategies used in avoidance maneuvers, an explicit expression of probability of collision in terms of relevant parameters is needed. The purpose of this work is to provide a method to calculate probability of collision expressed as an explicit function. Based on the formulation of the general method and the geometric features of the encounter described in Section 2.1, this approach will separately consider the probability of collision caused by differences in orbital altitude in the radial direction (Sect. 2.2.1), and the probability of collision caused by differences in arrival time in the cross section of the two objects (Sect. 2.2.2). Then the net probability of collision is obtained by multiplying the above two probabilities (Sect. 2.2.3). Numerical cases are listed to test this method in Section 3, and the conclusions are given in Section 4.

2 METHODOLOGY

2.1 Background and Foundation

According to the geometric features of the encounter that are shown in Figure 1, a collision between two space objects could only happen near the intersection of their orbital planes. Therefore, the differences in orbital altitude and arrival time when they are passing the intersection of their orbital planes can be used to predict dangerous encounters. The difference in orbital altitude is along the radial direction, and the difference in arrival time is determined by the velocities of motion in the cross section. If the cross section is perpendicular to the radial direction, the relative motion of two space objects can be divided into two independent parts, i.e., the radial motion and the motion within the cross section. Such a prerequisite is naturally satisfied for the encounter of two space objects in a near-circular orbit.

In this study, it is necessary to consider the eccentricity distribution exhibited by space objects. For space missions and spacecrafts that concern us, dangerous objects are in near earth orbits. Therefore, we select 13 000 space objects with altitudes of their perigee below 2000 km in a Two-Line Element set from NORAD. The eccentricity distribution for these space objects is shown in Figure 2. The overall eccentricity distribution is dominated by the small eccentricities, i.e., more than 90% of space objects are in near-circular orbits with eccentricities less than 0.1. Moreover, the eccentricity distribution also varies with altitude of perigee, and the fraction of large eccentricities increases with decreasing altitude. There are a few numbers concentrated around large values in the

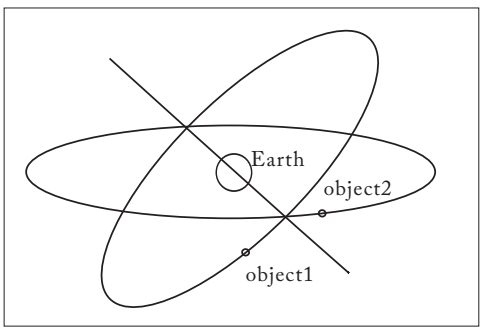

Fig. 1 Geometry of space objects during an encounter. When a close encounter happens, the two objects are both orbiting near the intersection of their orbital planes.

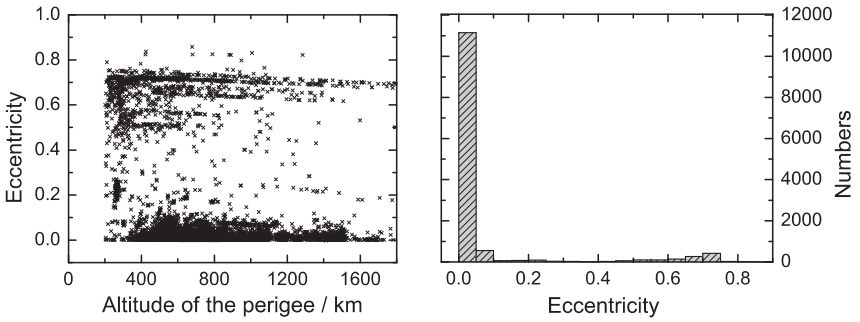

Fig. 2 Eccentricity distribution of space objects in a near-earth orbit below 2000 km. *Left*: Eccentricity distribution versus altitude of perigee. *Right*: Statistics of the eccentricity distribution.

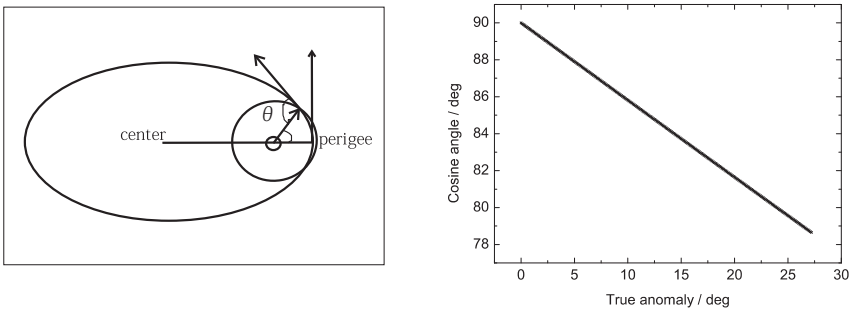

Fig. 3 Orthogonality between the radial direction and the motion direction for dangerous objects in an orbit with larger eccentricity. *Left*: Close encounter geometry for a satellite in a circular orbit with a dangerous object in an orbit with large eccentricity. The eccentricity is set as 0.7. θ, which we define as cosine angle here, is the included angle between the radial vector and the velocity vector. *Right*: The cosine angle between the radial direction and the velocity direction varies with the true anomaly.

eccentricity distribution ($0.5 \sim 0.8$), whose altitudes at perigee are only several hundred kilometers (mostly between 200 km and 800 km), as shown in the left panel. Objects in a highly eccentric orbit move faster and spend less time near the perigee. Therefore, most encounters happen between space objects that are in near-circular orbits.

However, a close encounter between a near-circular orbit below 2000 km and a highly eccentric orbit could only happen near the perigee. A sketch of such case is shown in the left panel of Figure 3, where the eccentricity of the elliptical orbit is 0.7. Obviously, at the point of perigee ($f = 0^\circ$), with cosine angle $\theta = 90^\circ$, the radial direction is orthogonal to the cross section. The right panel of Figure 3 shows that cosine angle θ varies with true anomaly f; θ equaling 90° indicates the vertical direction, and it can reach an extreme value of about a 12° deviation from vertical in this case. Actually, dangerous encounters between space objects in a highly eccentric orbit like this case rarely occur. Moreover, we can also predict the probability of encounters between these objects. A warning system that defines a difference in altitude to be less than 10 km and difference in time within 15 s is set to warn of dangerous encounters. Among these dangerous encounters, the direction cosine angles between the radial direction and the cross section are also calculated, and they are consistently approximately 90°.

Through the above analysis, it is reasonable to separate orbital motions in the radial direction from those in the cross section for most close encounters in a near-circular orbit. Based on this premise, we can separate the net probability of collision into two parts: one is in the radial direction which is caused by the difference in orbital altitude, and the other is in the cross section which is caused by the difference in the arrival time. The net probability of collision is derived by multiplying them together. The method for calculating probability of collision is appropriate for most encounters that occur in near-circular orbits.

2.2 Calculation Algorithms

2.2.1 The probability of collision in the radial direction

Firstly, assuming two space objects arrive at the intersection of their orbital planes at the same time, one has to only consider the relative trajectory and position error in the radial direction as shown in Figure 4. The uncertainty in the relative radial position is defined by a one-dimensional normal distribution with the form

$$\rho(r) = \frac{1}{2\sqrt{\pi}\sigma_r} \exp\left\{\frac{-(r-\Delta h)^2}{2\sigma_r^2}\right\}, \tag{6}$$

where Δh is the difference in altitude of the two objects, and the relative error in position in the radial direction is given by $\sigma_r^2 = \sqrt{\sigma_{1r}^2 + \sigma_{2r}^2}$.

Then the density function describing the probability of collision can be given by

$$F(r) = \frac{1}{2\sqrt{\pi}\sigma_r} \int_{-\infty}^{r} \exp\left\{\frac{-(r-\Delta h)^2}{2\sigma_r^2}\right\} \mathrm{d}r\,. \tag{7}$$

It can be substituted by an approximate expression with the form

$$F(r) = \frac{\exp\left[a(r-\Delta h)\right]}{1+\exp\left[a(r-\Delta h)\right]}, \qquad \text{where } a = \frac{4}{\sqrt{2\pi}\sigma_r}\,. \tag{8}$$

The result from this approximation is sufficiently accurate and does not introduce error greater than 2% (Liu et al. 2005).

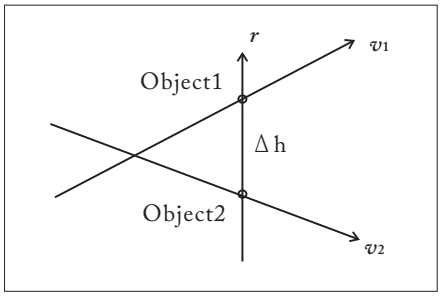

Fig. 4 The relative motion in the radial direction. When the two objects are arriving at the intersection of their orbital planes, the difference in orbital altitude is set to Δh.

Denoting the combined size of the objects in the radial direction as r_a, the probability of collision caused by difference in altitude can be expressed as

$$P_R \;=\; F(x)\,|_{-\infty}^{r_a} - F(x)\,|_{-\infty}^{-r_a} = \frac{\exp\left[\frac{4(r_a-\Delta h)}{\sqrt{2\pi}\sigma_r}\right]}{1+\exp\left[\frac{4(r_a-\Delta h)}{\sqrt{2\pi}\sigma_r}\right]} - \frac{\exp\left[\frac{4(-r_a-\Delta h)}{\sqrt{2\pi}\sigma_r}\right]}{1+\exp\left[\frac{4(-r_a-\Delta h)}{\sqrt{2\pi}\sigma_r}\right]}\,. \tag{9}$$

The probability of collision in the radial direction is reduced to an analytical expression in terms of difference in radial altitude, relative error and combined size.

2.2.2 The probability of collision in the cross section

The state vectors when the two objects reach the intersection of their orbital planes are labeled as: $\boldsymbol{r}_1, \boldsymbol{r}_2$ and $\boldsymbol{v}_1, \boldsymbol{v}_2$. We use a scale factor $\beta = r_1/r_2$ to eliminate the difference in radial altitude of the two objects, and thus only consider their relative motion in the cross section.

In order to compute the probability of collision in the cross section, the encounter coordinate frame is reconstructed as shown in Figure 5. The x' direction is normal to the cross section which is defined by the plane containing vectors $\boldsymbol{v}_1$ and $\boldsymbol{v}_2\beta$. The y' direction is defined as the position vector at CPA in the cross section. The z' vector completes the right-handed system. The $o' - x'y'z'$ system is centered on one object.

In the cross section, if the initial position and velocity vectors of two objects are respectively $\boldsymbol{r}_{10}, \boldsymbol{v}_{10}$ and $\boldsymbol{r}_{20}\beta, \boldsymbol{v}_{20}\beta$, the relative position vector between them is given by

$$\boldsymbol{\rho}(t) = (\boldsymbol{r}_{20}\beta - \boldsymbol{r}_{10}) + (\boldsymbol{v}_{20}\beta - \boldsymbol{v}_{10})t = \boldsymbol{\rho}_0 + \boldsymbol{r}_r t\,. \tag{10}$$

When the two objects are arriving at the CPA, the equation $\frac{\mathrm{d}}{\mathrm{dt}}[\boldsymbol{\rho}(t)\cdot\boldsymbol{\rho}(t)] = 0$ must be satisfied. We obtain the time of closest approach (TCA)

$$t_{\mathrm{CPA}} = -\frac{\boldsymbol{\rho}_0\cdot\boldsymbol{v}_r}{\boldsymbol{v}_r\cdot\boldsymbol{v}_r}\,. \tag{11}$$

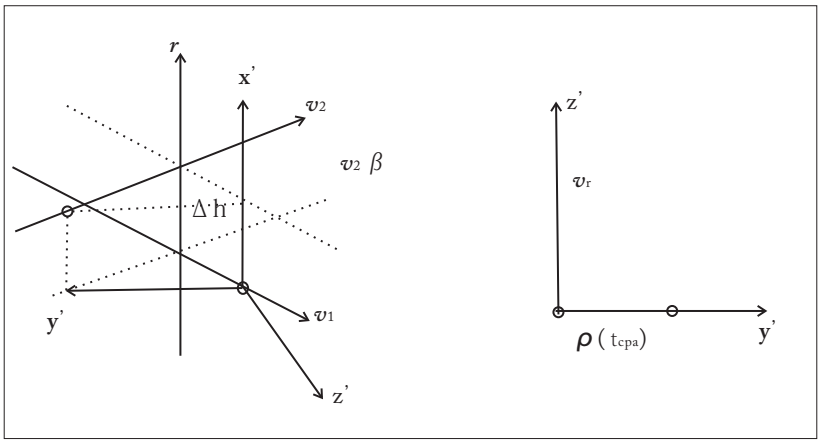

Fig. 5 The reconstructed encounter frame. The x' direction is normal to the cross section. The y' direction is defined as the position vector at CPA in the cross section. The z' vector completes the right-handed system.

Then the vector defined by the CPA is given by

$$\boldsymbol{\rho}(t_{\mathrm{CPA}}) = \boldsymbol{\rho}_0 + \Big(\frac{-\boldsymbol{\rho}_0 \cdot \boldsymbol{v}_r}{\boldsymbol{v}_r \cdot \boldsymbol{v}_r}\Big)\boldsymbol{v}_r \,. \tag{12}$$

Therefore, unit vectors of the reconstructed encounter frame can be defined by:

$$\begin{aligned} \hat{x}' &= \tfrac{\boldsymbol{v}_1 \times \boldsymbol{v}_2 \beta}{|\boldsymbol{v}_1 \times \boldsymbol{v}_2 \beta|} \,, \\ \hat{y}' &= \tfrac{\boldsymbol{\rho}(t_{\mathrm{CPA}})}{|\boldsymbol{\rho}(t_{\mathrm{CPA}})|} \,, \\ \hat{z}' &= \hat{x}' \times \hat{y}' \,. \end{aligned} \tag{13}$$

Based on the foundation described in Section 2.1, the $\hat{x}'$ axis is basically parallel to the radial direction at the intersection of the orbital planes. The transformation from the inertial frame to the reconstructed encounter frame is defined to separate the radial motion from the cross section by directly eliminating motion in the x' direction. At the same time, there is no uncertainty in the direction of relative velocity at TCA in the cross section, so the relative position error can be projected into the direction of the vector at CPA. After projecting the combined size of the objects into the direction of the vector at CPA, the probability of collision caused by a difference in the arrival time in the cross section is given by

$$P_T = \frac{1}{2\sqrt{\pi}\sigma_t} \int_{-r_t}^{r_t} \exp\left\{\frac{-(y-\rho_{\min})^2}{2\sigma_t^2}\right\} \mathrm{d}y \,, \tag{14}$$

where σ_t is defined as the relative position error along the direction of the vector at CPA, and it only depends on position errors in the directions of along-track and normal to the track. $\rho_{\min}$ is the distance at CPA in the cross section. r_t is the combined size along the direction of the vector at CPA in the cross section.

Similarly, by using the approximate expression we can also obtain an analytical solution:

$$\begin{aligned} P_T &= F(x)\,|_{-\infty}^{r_t} - F(x)\,|_{-\infty}^{-r_t} \\ &= \frac{\exp\left[\frac{4(r_t-\rho_{\min})}{\sqrt{2\pi}\sigma_t}\right]}{1+\exp\left[\frac{4(r_t-\rho_{\min})}{\sqrt{2\pi}\sigma_t}\right]} - \frac{\exp\left[\frac{4(-r_t-\rho_{\min})}{\sqrt{2\pi}\sigma_t}\right]}{1+\exp\left[\frac{4(-r_t-\rho_{\min})}{\sqrt{2\pi}\sigma_t}\right]} \,. \end{aligned} \tag{15}$$

2.2.3 The net probability of collision as an explicit function

In the above two subsections, we separately obtain analytical expressions of probability of collision caused by differences in altitude and time. Collision events can only happen when the two probabilities are big enough at the same time. Therefore, the net probability of collision between two space objects can be defined by:

$$\begin{aligned} P &= P_R \cdot P_T \\ &= \left\{ \frac{\exp\left[\frac{4(r_a-\Delta h)}{\sqrt{2\pi}\sigma_r}\right]}{1+\exp\left[\frac{4(r_a-\Delta h)}{\sqrt{2\pi}\sigma_r}\right]} - \frac{\exp\left[\frac{4(-r_a-\Delta h)}{\sqrt{2\pi}\sigma_r}\right]}{1+\exp\left[\frac{4(-r_a-\Delta h)}{\sqrt{2\pi}\sigma_r}\right]} \right\} \\ &\quad \cdot \left\{ \frac{\exp\left[\frac{4(r_t-\rho_{\min})}{\sqrt{2\pi}\sigma_t}\right]}{1+\exp\left[\frac{4(r_t-\rho_{\min})}{\sqrt{2\pi}\sigma_t}\right]} - \frac{\exp\left[\frac{4(-r_t-\rho_{\min})}{\sqrt{2\pi}\sigma_t}\right]}{1+\exp\left[\frac{4(-r_t-\rho_{\min})}{\sqrt{2\pi}\sigma_t}\right]} \right\} . \end{aligned} \tag{16}$$

This method gives an explicit expression to compute probability of collision. It is advantageous to directly analyze the factors that influence the probability of collision. Additionally, the method separates orbital motions in the radial direction from those in the cross section. Therefore, position errors and geometric sizes of the two components can be handled differently to improve precision, especially for irregularly shaped spacecrafts, such as shuttles with wings.

3 NUMERICAL RESULTS AND DISCUSSION

A computer program has been developed to implement the technique and test cases have been run. Firstly, a collision accident between two items of space debris, which happened on 2005 January 17, is applied. State vectors of the two items of debris in the inertial system are listed in Table 1. The radius of the combined geometric sphere is set to 100 m. The method in this paper described in Equation (16) and the general method described in Equation (5) are respectively implemented to compute probability of collision.

Table 1 State Vectors in the Inertial Frame

Number	x (km)	y (km)	z (km)	v_x (km s^{-1})	v_y (km s^{-1})	v_z (km s^{-1})
07219	–150.798	1182.677	–7143.776	7.290	–1.126	–0.354
26202	–150.620	1182.018	–7143.788	5.915	4.348	0.643

Figure 6 displays the variation in probability of collision versus the relative position error in the along-track direction. In the left panel of Figure 6, the ratio of position errors along three principle axes in the local frame is set to be 1: 1: 1, and it is 1: 5: 1 for the right panel. We can see that the results essentially show agreement between our method and the general method, with our method being a little larger than the general case. Actually, the tiny deviation is caused by the integrated area from a circle with diameter $2r$ changing to a square with the length of each side being $2r$. However, this makes no significant difference for assessment of risk related to probability of collision.

The Center for Space Standards and Innovation (CSSI) offers Satellite Orbital Conjunction Reports Assessing Threatening Encounters in Space (SOCRATES) which lists the top ten threatening encounters ordered by minimum range over the next seven days. Based on the orbital data listed in SOCRATES on 2013 March 13, we assess the risk of collision between the two objects that were involved. The time of CPA and the minimum distance between the two objects are calculated, and results from the probability of collision derived from both our method and the general method are listed in Table 2. The results show that the probabilities of collision from our method are on the same order of magnitude compared with the general method. Therefore, the probability of collision from the method in this paper is credible for assessing the risk of collision.

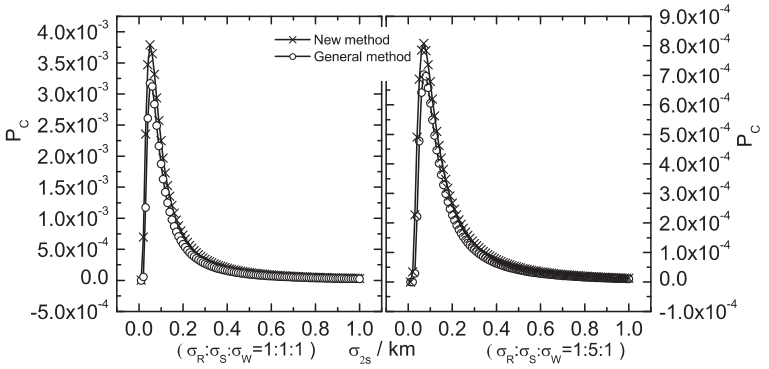

Fig. 6 Variation in probability of collision versus the relative position error. The ratio of position error along three principle axes in the local frame is set to be 1: 1: 1 for the left panel, and 1: 5: 1 for the right panel. (Probabilities of collision related to this case are also calculated in papers by other authors (Bai & Chen 2008); the maximum probability corresponding to the right panel is 7.12×10^{-3}).

Table 2 Probability of Collision Results

Catalog Number	TCA (UTC)	Min Range (km)	Position Error (km)	General Method	This Method
25415&31445	Mar 18 14:44:34	0.115	0.128	1.24×10^{-5}	1.52×10^{-5}
20737&20738	Mar 17 10:39:31	0.104	0.380	1.70×10^{-6}	2.15×10^{-6}
27939&31588	Mar 16 13:46:21	0.098	0.073	3.01×10^{-5}	3.51×10^{-5}
11308&32315	Mar 15 03:02:16	0.094	0.107	1.80×10^{-5}	2.05×10^{-5}
17583&37442	Mar 16 14:02:50	0.039	0.011	9.39×10^{-5}	1.88×10^{-4}

4 CONCLUSIONS

The existing general method for calculating the probability of collision provides sufficiently accurate results, but is not based on a direct connection between the probability of collision, the geometry of the encounter and the related error covariance. Based on the geometry of the encounter, a method is developed to compute probability of collision. This method gives an explicit expression to compute probability of collision which is expressed as a function of the radial and the cross section components of the relative position and error covariance. The expression is compact and advantageous for directly analyzing the factors that influence the probability of collision. A computer program is developed to implement the technique, and the results of calculations are compared with the general method, which show that this method is applicable to most situations where assessing the risk of collision in a near-circular orbit is required. Additionally, the method separates orbit motions in the radial direction from those in the cross section. Therefore, position errors and geometric sizes of the two components can be handled differently to improve precision, especially for irregularly shaped spacecrafts, such as shuttles with wings. Continuation of this work is currently in progress.

Acknowledgements This work was funded by the National Natural Science Foundation of China (Grant No. 11203085).

References

Akella, M. R., & Alfriend, K. T. 2000, Journal of Guidance Control Dynamics, 23, 769

Bai, X. Z., & Chen, L. 2008, Journal of Astronautics, 29, 1435

Bai, X. Z., & Chen, L. 2009, Chinese Journal of Space Science, 29, 422

Chan, K. 1997, Advances in Astronautical Sciences, 96, 1033 (*http://rep157.infoeach.com/view-MTU3 fDIxO-TYzNTM=.html*)

Francois, L., & Eloy, S. 2008, Space Operations Communicator, 5

Kelly, B. D., & Picciotto, S. D. 2005, AIAA 2005-6775 (*http://debris-spatiaux.cnes.fr /articles/LFES1114681.pdf*)

Klinkrad, H., Alarcon, J. R., & Sanchez, N. 2005, in 4th European Conference on Space Debris (ESA Special Publication), 587, ed. D. Danesy, 509

Leleux, D., Spencer, R., Zimmerman, P., et al. 2002, in Space OPS 2002 Conference, Houston TX, USA

Liu, Q. J., Chen, T., Chen, S. C., & Liu, Q. 2005, Advanced Measurement and Laboratory Management, 3, 21

Patera, R. P. 2001, Journal of Guidance Control Dynamics, 24, 716

Sun, R.-Y., & Zhao, C.-Y. 2013, RAA (Research in Astronomy and Astrophysics), 13, 604